PHYSICAL REVIEW B VOLUME 10, NUMBER 8 15 OCTOBER 1974

Vacancy-vacancy, vacancy-impurity, and impurity-impurity interactions in aluminum

Osamu Takai, Ryoichi Yamamoto, Masao Doyama, and Yoshihiro Hisamatsu
Department of Metallurgy and Materials Science, Faculty of Engineering, The University of Tokyo, Bunkyo-ku, Tokyo 113, Japan
(Received 1 April 1974)

Electronic interactions between vacancies and impurity atoms have been generally studied using the pseudopotential formulation based on the second-order perturbation theory. The distortions of the lattice around vacancies and impurity atoms were conventionally neglected because of their great complexity. The vacancy-vacancy, vacancy-impurity, and impurity-impurity interaction potentials have been calculated in aluminum using three kinds of exchange and correlation corrections in the dielectric function of the conduction electrons. They all show the long-range oscillatory behavior. The binding energies of a divacancy, fifteen kinds of vacancy-impurity pairs, and eighteen kinds of impurity-impurity pairs have been also calculated. The results indicate small binding energies, which are generally well consistent with recent experiments and the theoretical results previously obtained from the electrostatic model based on the screening potentials. The interaction potentials have been applied to the study of small point-defect clusters, for which the configurations and binding energies have been discussed. The random-phase approximation is also found to give less reliable results. Therefore the appropriate including of many-electron effects is essential in obtaining realistic results.

I. INTRODUCTION

A great number of quenching, equilibrium, diffusion, and positron-annihilation experiments on pure metals and dilute alloys have shown that the point defects and their interactions play an important role in these experiments, while the fundamental understanding is not sufficient. Both experimental and theoretical studies have been reviewed recently on point defects and the interactions between them in metals.[1-3] The binding energies of a divacancy and vacancy-impurity pairs in aluminum have been experimentally obtained by various methods. The experimental values, however, differ from one another and have not been settled on account of experimental difficulties. Few experiments on the impurity-impurity interaction have been studied. Perry[4] analyzed the results of Takamura[5] on quenched dilute Al-Zn alloys including this interaction.

Two major factors in the interaction between point defects are the elastic interaction or the distortion of the lattice around them[6] and the electronic interaction.[7] These two factors cannot be essentially separated from each other, but the total interactions between point defects have been often considered as the sum of them. The elastic interaction is not such a simple problem as can be treated by the elastic theory of the continuum and is very difficult to treat in a complete form at present. The method of lattice statics[8-14] or the Green's-function method[15,16] may overcome this difficulty. The electronic interaction has been extensively studied, using the screening potentials, by many authors[17] since Lazarus. One of the main conclusions of these studies is that the electronic interaction energies in aluminum are likely to be very small, which is in good agreement with recent experiments. However, the electrostatic model based on the screening potential is unsatisfactory for the following reasons: (i) The impurity atom is only characterized by its valence. (ii) The electronic structure of conduction electrons in a metal is not appropriately included in the theory. (iii) Vacancy-impurity and impurity-impurity interaction energies vanish for homovalent impurity atoms which have the same valence as a host atom.

In recent years various properties of metals have been successfully treated by the pseudopotential theory.[18] Most of the recent calculations on the properties of point defects use effective interionic potentials constructed according to the pseudopotential theory.[19] The vacancy-vacancy, vacancy-impurity, and impurity-impurity interactions have been generally treated,[20-22] within the framework of the pseudopotential method based on the second-order perturbation theory, extending the structural approach initiated by Harrison.[23] The total lattice energy can be separated into volume-dependent and structure-dependent energies in the pseudopotential theory. In the above treatment, only the structural energies are calculated under the condition of constant volume and the lattice distortions around vacancies and impurity atoms are neglected because of their great complexity. We wish to remark that this treatment improves the electrostatic model discussed above and that the effective interaction potential between point defects can be described by a pairwise central interaction between them similar to the interionic potential. The pairwise interaction consists of a direct Coulomb interaction and an indirect interaction due to the screening by the conduction electrons which depends on the pseudopotential form factors and the

dielectric function.

In this paper, we report the detailed numerical results of the electronic interactions between vacancies and impurity atoms in aluminum. The reliability of different correction factors to exchange and correlation effects of the conduction electrons in the dielectric function is also compared. For this purpose, we use form factors constructed by the same bare-ion pseudopotential but screened by three different dielectric functions. We discuss the effective interaction potentials between point defects, i.e., vacancies themselves, a vacancy and an impurity atom, and impurity atoms themselves, in Sec. II, and the binding energies between them in Sec. III. We also discuss the configurations and binding energies of the small point-defect clusters as an application of the effective interaction potentials, in Sec. IV. Conclusions are presented in Sec. V.

II. EFFECTIVE INTERACTION POTENTIALS BETWEEN POINT DEFECTS

We denote a host atom by H, a vacancy by V, and two kinds of substitutional impurity atoms by A and B. The various effective interaction potentials between them can be written as follows[20–22]:

$$\phi_{VV}(R) = \frac{Z_H^2 e^2}{R} + \frac{\Omega_H}{\pi^2}\int_0^\infty q^2 \frac{\sin qR}{qR} F_{HH}(q)\, dq, \tag{1}$$

$$\phi_{VA}(R) = -\frac{Z_H \Delta Z_A e^2}{R} + \frac{\Omega_H}{\pi^2}\int_0^\infty q^2 \frac{\sin qR}{qR} \times [F_{HH}(q) - F_{HA}(q)]\, dq\ , \tag{2}$$

$$\phi_{AA}(R) = \frac{\Delta Z_A^2 e^2}{R} + \frac{\Omega_H}{\pi^2}\int_0^\infty q^2 \frac{\sin qR}{qR} \times [F_{HH}(q) + F_{AA}(q) - 2F_{HA}(q)]\, dq\ , \tag{3}$$

$$\phi_{AB}(R) = \frac{\Delta Z_A \Delta Z_B e^2}{R} + \frac{\Omega_H}{\pi^2}\int_0^\infty q^2 \frac{\sin qR}{qR} \times [F_{HH}(q) + F_{AB}(q) - F_{HA}(q) - F_{HB}(q)]\, dq\ , \tag{4}$$

where R is the distance between two kinds of point defects, $\Delta Z_A = Z_A - Z_H$ and $\Delta Z_B = Z_B - Z_H$. $F_{\alpha\beta}(q)$ is the energy–wave-number characteristic defined by

$$F_{\alpha\beta}(q) = w_\alpha(q) w_\beta(q) \chi_H(q) \epsilon_H(q)\ , \tag{5}$$

where $w_\alpha(q)$ and $w_\beta(q)$ are the form factors of atom α and atom β, respectively. The form factor of an impurity atom in a host metal will be discussed later. $\chi_H(q)$ and $\epsilon_H(q)$ are the perturbation characteristic and the dielectric function of a host metal given by

$$\chi_H(q) = -\tfrac{1}{2} Z_H \left(\tfrac{2}{3} E_F^H\right)^{-1} \times \left(\frac{1}{2} + \frac{4(k_F^H)^2 - q^2}{8 q k_F^H} \ln\left|\frac{q + 2k_F^H}{q - 2k_F^H}\right|\right), \tag{6}$$

and

$$\epsilon_H(q) = 1 - \frac{8\pi e^2}{\Omega_H q^2}[1 - f(q)]\chi_H(q)\ , \tag{7}$$

respectively, where $f(q)$ is the correction factor for exchange and correlation effects of the conduction electrons. The vacancy-vacancy interaction $\phi_{VV}(R)$ is just the same as the host-host interaction $\phi_{HH}(R)$, which has been shown by Harrison.[23] $\phi_{VB}(R)$ and $\phi_{BB}(R)$ are given similar to $\phi_{VA}(R)$ and $\phi_{AA}(R)$, respectively. All the effective interaction potentials consist of two terms. The first is the direct Coulomb interaction between the excess charges of point defects; the second is the indirect interaction due to the screening by the conduction electrons in a metal.

On the numerical calculation of these potentials, the choice of the bare-ion pseudopotential, that of the exchange and correlation correction $f(q)$, and the type of the impurity form factor in a host metal are considerably important. For the bare-ion pseudopotential, we use the empty core model potential of Ashcroft[24] given by

$$v(q) = -(4\pi Z e^2/\Omega q^2)\cos(qR_c)\ , \tag{8}$$

where R_c is an adjustable parameter representing an effective radius of the ion core in a metal. The core radii R_c used[25] are listed in Table II. This form has been successfully used as the bare-ion pseudopotential in studying many properties of metals for its simplicity.

The correction function $f(q)$ in Eq. (7) has been extensively investigated by many authors. Various forms of $f(q)$ have been proposed for approximating the many-electron effects. In the present calcula-

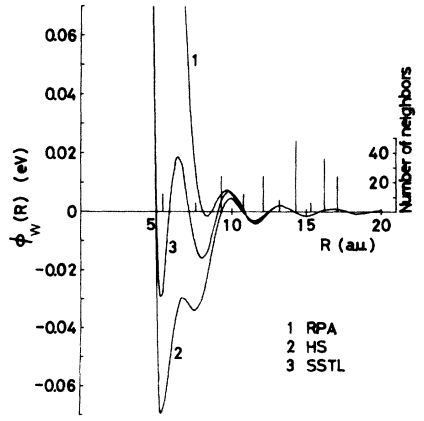

FIG. 1. Vacancy-vacancy interaction potentials in aluminum. RPA, HS, and SSTL denote the correction factors $f(q)$ used. The vertical bars indicate the positions and the numbers up to the tenth neighbor.

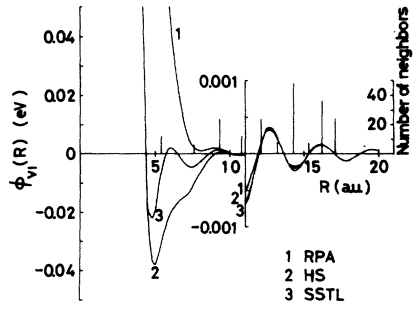

FIG. 2. Vacancy–Zn-impurity interaction potentials in aluminum.

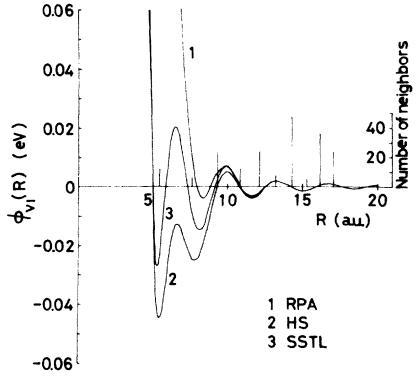

FIG. 4. Vacancy–Cu-impurity interaction potentials in aluminum.

tions, three different forms are used for comparison:

1. *Random-phase approximation (referred to as* RPA). $f(q)$ is simply given by

$$f(q) = 0 \ . \tag{9}$$

2. *Hubbard-Sham approximation (referred to as* HS). The Hubbard-Sham approximation[26] includes only the exchange effects. $f(q)$ is given by

$$f(q) = q^2/2(q^2 + k_F^2 + k_s^2) \ , \tag{10}$$

where k_s is the screening parameter taken as $(2k_F/\pi)^{1/2}$.[27]

3. *Singwi et al. approximation (referred to as* SSTL). Singwi *et al.*[28] have recently included both Coulomb correlation and exchange effects based on a self-consistent screening theory. The analytic form is given by

$$f(q) = A\{1 - \exp[-B(q/k_F)^2]\} \ . \tag{11}$$

The constants A and B have a weak dependence on the interelectronic spacing r_s and are taken to be $A = 0.9048$ and $B = 0.3363$ for aluminum.

For convenience of comparison, we shall not change the bare-ion pseudopotential throughout the calculation. As for the impurity form factor in a host atom, we use the following form[29]:

$$w_A(q) = \frac{\Omega_A \epsilon_A(q)}{\Omega_H \epsilon_H(q)} w_A^0(q) \ ,$$
$$w_B(q) = \frac{\Omega_B \epsilon_B(q)}{\Omega_H \epsilon_H(q)} w_B^0(q) \ , \tag{12}$$

where $w_A^0(q)$ and $w_B^0(q)$ are the form factors of impurity atoms in their pure state. This form was successfully used in the calculation of the electrical resistivity due to impurity atoms[30,31] and confirmed as a good approximation for alloying by Taut and Paash.[32]

We particularly select Zn, Mg, Cu, and Sn as the impurity atoms and Zn-Mg, Cu-Sn, and Cu-Mg as different impurity-impurity pairs, since they are known to be the important components of useful

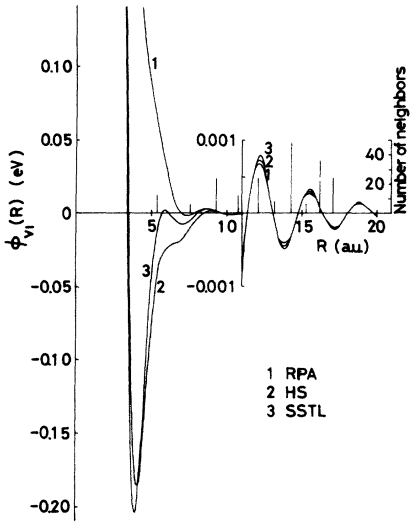

FIG. 3. Vacancy–Mg-impurity interaction potentials in aluminum.

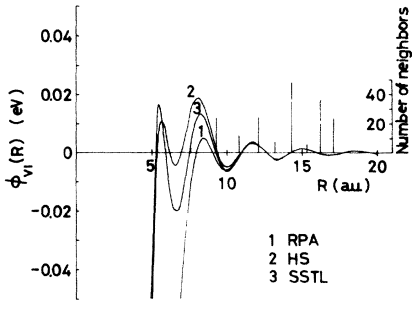

FIG. 5. Vacancy–Sn-impurity interaction potentials in aluminum.

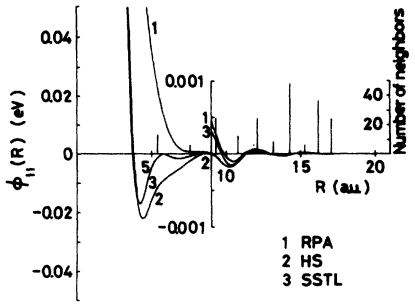

FIG. 6. Zn-impurity–Zn-impurity interaction potentials in aluminum.

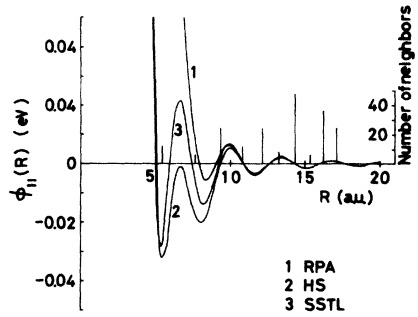

FIG. 8. Cu-impurity–Cu-impurity interaction potentials in aluminum.

commercial aluminum alloys. In Fig. 1 we plot the vacancy-vacancy interaction potentials using three different kinds of exchange and correlation corrections. The vacancy-impurity interaction potentials are plotted in Figs. 2–5 for four kinds of selected impurity atoms. The impurity-impurity interaction potentials are plotted in Figs. 6-12 for seven kinds of impurity-impurity pairs. All the effective interaction potentials between these point defects show the long-range oscillatory behavior but the interaction energies are generally very small especially farther than first few neighbor distances. The existence of the oscillating tail arises from the singular behavior of the dielectric screening. The vacancy-vacancy interaction potential is exactly equal to the effective interionic potential of aluminum, which has been calculated by many authors.[33] The long-range oscillatory nature of the vacancy-vacancy interaction was previously studied by Flynn[34] in noble metals. The influence of the exchange and correlation effects on the nature and the behavior of the interaction potentials is clearly a major one. It is seen that in the RPA case there is a significant change in the shape of the potentials corresponding to the first few neighbor distances; the potentials have no minimum or maximum in the region near the nearest-neighbor position except the interaction between a Mg-Mg impurity pair. The discrepancies between the potentials based on the HS correction and those based on the SSTL one would be somewhat less serious if the core radius were optimized in each case. However, three different kinds of potentials all have similar long-range oscillations beyond the fifth-neighbor position and the magnitude of these oscillations is almost less than 0.001 eV in each interaction. This shows that the long-range electronic interaction should be quite similar but not significant in contributing to defect binding energies. The obtained vacancy-impurity and impurity-impurity potentials may be most reliable for a Zn impurity atom, since Zn has nearly the same atomic radius as Al and so the effect of the lattice distortion is expected to be small. They are probably less reliable for a Cu impurity atom, because

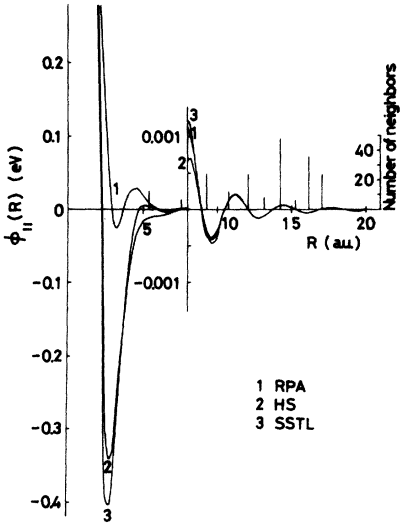

FIG. 7. Mg-impurity–Mg-impurity interaction potentials in aluminum.

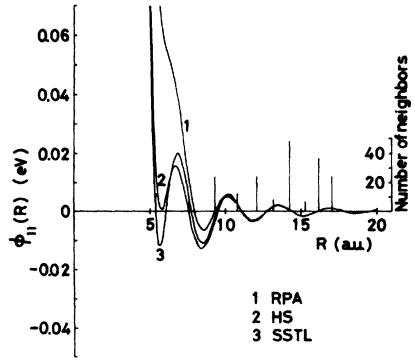

FIG. 9. Sn-impurity–Sn-impurity interaction potentials in aluminum.

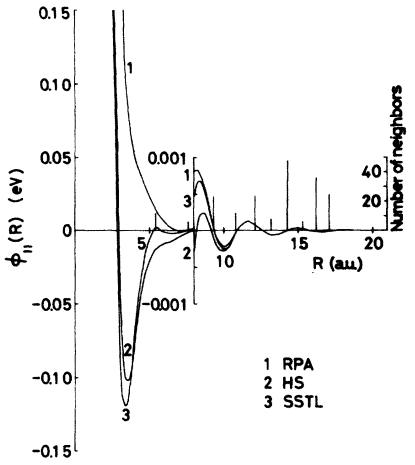

FIG. 10. Zn-impurity–Mg-impurity interaction potentials in aluminum.

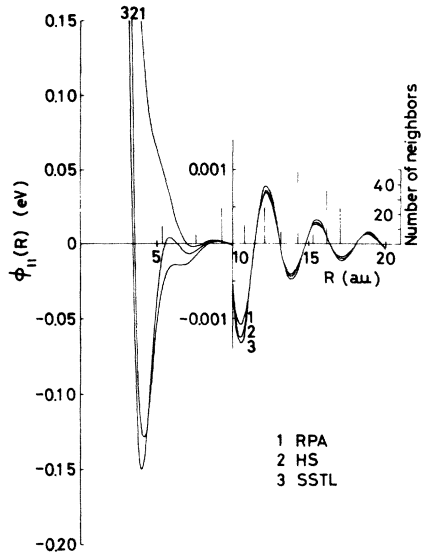

FIG. 12. Cu-impurity–Mg-impurity interaction potentials in aluminum.

the atomic radius of Cu is smaller than that of Al and the pseudopotential theory has been less successful for noble metals. The shapes of the vacancy–Sn-impurity and Cu-impurity–Sn-impurity interaction potentials are different from those of the other potentials. At present, we have no satisfactory explanation for these behavior in relation to the experimental results. The effective interaction potentials between vacancies and impurity atoms are very important in studying many properties of point defects. The obtained potentials will be applied in Sec. IV.

III. BINDING ENERGIES BETWEEN POINT DEFECTS

In Table I, we show the binding energies of a divacancy up to the fifth-neighbor positions. Negative binding energies denote the repulsive interaction hereafter. The divacancy binding energy obtained from the RPA is completely contrary to the experimental results. The energies obtained from other two cases including the many-electron effects are in good agreement with those obtained by Harrison.[23] They, however, are smaller than the experimental value of 0.17 ± 0.05 eV given by Doyama and Koehler.[35] A large part of this discrepancy probably resides in our neglect of the distortion of lattice around a divacancy.

The differences in the behavior of quenched-in vacancies in pure metals compared to alloys are largely due to the fact that vacancies and alloy atoms form pairs bound together with appropriate binding energies. As a result, the equilibrium vacancy concentrations can be greatly increased, since the effective formation energy of the vacancies is decreased by the binding energy to the alloy or impurity atoms. This effect has a considerable technological importance, because it greatly influences age hardening behavior. The vacancy-impurity binding energies at nearest-neighbor positions are presented in Table II for 15 kinds of impurity atoms. We also show only the experimental values which have been obtained from the equilibrium experiments, because the vacancy-impurity binding energies obtained from quenching and aging studies are considered to be less reliable than those obtained from high-temperature equilibrium measurements as pointed out by Peterson and Rothman.[39] The values obtained from quenching and aging experiments are generally large; on the other hand, the values obtained from equilibrium experiments are small. The recent impurity diffusion experiments support small vacancy-impurity binding energies in aluminum for

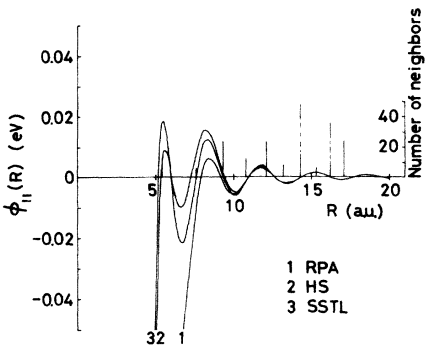

FIG. 11. Cu-impurity–Sn-impurity interaction potentials in aluminum.

TABLE I. Binding energies of a divacancy up to fifth-neighbor positions in aluminum (eV).

Neighbor	Correction factor $f(q)$ RPA	HS	SSTL	Harrison (Ref. 23)	Expt. (Ref. 35)
1st	−0.365	0.069	0.028	0.05	0.17±0.05
2nd	−0.012	0.034	0.013	0.013	
3rd	−0.006	−0.001	−0.004	−0.004	
4th	0.000	0.001	0.000	0.001	
5th	0.002	0.002	0.003	0.004	
Infinite Separation	0	0	0	0	

non-transition-impurity atoms. As regards the calculated values, the binding energies using the RPA are also quite contrary to the experimental results. However, the binding energies using the HS and SSTL correction factors are very small, which is well consistent with the recent experiments and the previous theoretical results obtained from the electrostatic model. Moreover, it is very interesting to note that the vacancy–Zn-impurity binding energy of 0.031 eV (HS) or 0.007 eV (SSTL) is almost the same value as that of 0.019± 0.004 eV estimated recently by Snead *et al.*[40] from the positron-annihilation experiment. This fact suggests that the elastic interaction or the effect of lattice relaxation may be small and of the same order as the electronic interaction for this case. The small negative binding energy between a vacancy and a Sn impurity atom is notable, since the vacancy–Sn-impurity binding energy has been considered to be particularly large[41]; but Suzuki *et al.*[42] have recently estimated it to be less than or, at most, equal to the vacancy–Cu-impurity binding energy. We have recently found the relationships between the vacancy-impurity binding energy and the core radius, the Debye temperature, and the melting temperature in aluminum.[43]

Some impurity atoms are known to form Guinier-Preston (GP) zones in aluminum. Thus, appreciable impurity-impurity binding must exist in these alloys. Perry[4] has shown that the results of Takamura[5] on quenched dilute Al-Zn alloys (up to 0.42-at.% Zn) cannot be explained by a single vacancy-impurity binding energy but an appropriate impurity-impurity binding energy is needed to fit the results. In Table III, the binding energies of impurity-impurity pairs at adjacent lattice sites are given for 18 kinds of impurity pairs. The binding energies obtained from the RPA may be unreliable, since those between the same impurity pairs all show the repulsive interaction which is inconsistent with the above discussion. As to the HS and SSTL cases, the binding energies are generally small and

TABLE II. Vacancy-impurity binding energies at nearest-neighbor positions in aluminum (R_c =1.12 a.u.) (eV). Also shown are the core radii R_c used (Ref. 25), the relative values of the atomic radius R_a to that of aluminum (R_a=2.984 a.u.), and the valences of impurity atoms.

Impurity	R_c (a.u.)	R_a	Z	Correction factor $f(q)$ RPA	HS	SSTL	Equilibrium experiments
Li	1.06	1.09	1	−0.248	0.045	0.020	
Na	1.67	1.32	1	−0.166	0.083	0.034	
K	2.11	1.63	1	−0.025	0.192	0.123	
Rb	2.12	1.74	1	−0.021	0.195	0.127	
Cs	2.16	1.89	1	−0.002	0.211	0.141	
Cu	0.81	0.89	1	−0.263	0.045	0.027	~0[a]
Ag	1.04	1.01	1	−0.249	0.045	0.020	0.08[b]
Au	0.81	1.01	1	−0.263	0.045	0.027	
Mg	1.39	1.12	2	−0.064	0.042	0.009	0[c]
Zn	1.27	0.97	2	−0.093	0.031	0.007	
Hg	0.915	1.12	2	−0.150	0.020	0.019	
In	1.32	1.16	3	0.059	0.018	−0.004	
Sn	1.30	1.18	4	0.192	−0.003	−0.015	
Pb	1.47	1.22	4	0.282	0.038	−0.001	
Bi	1.49	1.29	5	0.460	0.038	−0.004	

[a]Reference 36. [b]Reference 37. [c]Reference 38.

TABLE III. Impurity-*A*–Impurity-*B* binding energies at nearest-neighbor positions in aluminum (eV).

Impurity		Correction factor $f(q)$		
A	*B*	RPA	HS	SSTL
Li	Li	−0.168	0.030	0.014
Na	Na	−0.084	0.050	0.005
K	K	−0.066	0.000	−0.079
Rb	Rb	−0.066	−0.002	−0.082
Cs	Cs	−0.070	−0.014	−0.097
Cu	Cu	−0.186	0.032	0.027
Ag	Ag	−0.170	0.030	0.015
Au	Au	−0.186	0.032	0.027
Mg	Mg	−0.011	0.010	−0.004
Zn	Zn	−0.023	0.011	0.001
Hg	Hg	−0.056	0.009	0.016
In	In	−0.007	−0.009	−0.004
Sn	Sn	−0.095	−0.017	0.002
Pb	Pb	−0.230	−0.134	−0.084
Bi	Bi	−0.607	−0.273	−0.165
Zn	Mg	−0.015	0.013	0.000
Cu	Sn	0.133	−0.003	−0.017
Cu	Mg	−0.050	0.028	0.006

TABLE V. Impurity-*A*–Impurity-*B* binding energies from the second- to the fifth-neighbor positions using the SSTL correction factor in aluminum (eV).

Impurity		Neighbor			
A	*B*	2nd	3rd	4th	5th
Li	Li	0.006	−0.002	0.000	0.001
Na	Na	0.006	−0.002	0.001	0.000
K	K	0.012	−0.006	0.003	−0.001
Rb	Rb	0.012	−0.006	0.003	−0.001
Cs	Cs	0.013	−0.006	0.003	−0.001
Cu	Cu	0.007	−0.002	−0.001	0.003
Ag	Ag	0.006	−0.002	0.000	0.002
Au	Au	0.007	−0.002	−0.001	0.003
Mg	Mg	−0.001	0.000	0.000	0.000
Zn	Zn	0.001	0.000	0.000	0.000
Hg	Hg	0.001	−0.001	−0.001	0.002
In	In	−0.003	0.001	−0.001	0.001
Sn	Sn	−0.003	0.001	−0.003	0.003
Pb	Pb	−0.016	0.007	−0.008	0.007
Bi	Bi	−0.025	0.013	−0.015	0.015
Zn	Mg	0.000	0.000	0.000	0.000
Cu	Sn	−0.002	0.000	0.002	−0.003
Cu	Mg	0.005	−0.002	0.001	−0.001

there exist the attractive interactions between impurity atoms which form GP zones. This is in reasonable agreement with experiments. The calculated values are also well consistent with the theoretical calculations by Blandin and Déplanté[44] using the self-consistent screening potential. Concerning the different impurity pairs, the binding energy was found for Zn-Mg or Cu-Mg, but for Cu-Sn the negative binding energy was found at the nearest-neighbor positions. It is difficult to conclude the physical meaning of this behavior from only the electronic binding energies as the lattice distortions were neglected.

The vacancy-impurity and impurity-impurity binding energies from the second- to the fifth-neighbor positions using the SSTL correction factor are presented in Tables IV and V, respectively. As seen from these tables, the magnitude of binding energies at the farther-neighbor positions is almost much smaller than that at the nearest-neighbor positions. It is noted that the attractive interaction was found at the second-, third-, or fourth-neighbor positions in spite of the repulsive interaction at the nearest-neighbor positions. This behavior is important to the clustering of impurity atoms.

TABLE IV. Vacancy-impurity binding energies from the second- to the fifth-neighbor positions using the SSTL correction factor in aluminum (eV).

	Neighbor			
Impurity	2nd	3rd	4th	5th
Li	0.009	−0.003	0.000	0.002
Na	0.010	−0.004	0.001	0.000
K	0.014	−0.006	0.002	0.001
Rb	0.015	−0.006	0.002	0.001
Cs	0.015	−0.006	0.002	0.001
Cu	0.010	−0.003	0.000	0.003
Ag	0.009	−0.003	0.000	0.002
Au	0.010	−0.003	0.000	0.003
Mg	0.005	−0.002	0.001	−0.001
Zn	0.004	−0.001	0.001	0.000
Hg	0.005	−0.002	−0.001	0.002
In	0.000	0.000	0.001	−0.002
Sn	−0.004	0.001	0.001	−0.003
Pb	−0.002	0.000	0.003	−0.005
Bi	−0.006	0.001	0.004	−0.007

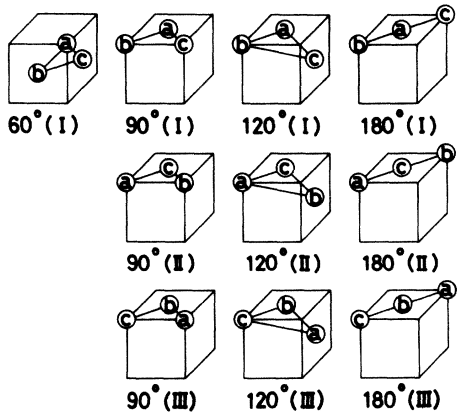

FIG. 13. General configurations of small point-defect clusters containing three kinds of point defects, *a*, *b*, and *c*.

TABLE VI. Binding energies of various trivacancies in aluminum (eV). Binding energies are given as the ratios to the binding energy of the 60° (I) type. Also shown are the ratios of binding energies to the divacancy binding energy in parentheses and the relative ratios obtained by Doyama and Cotterill (Ref. 46) in copper using a Morse potential function.

Type	Correction factor $f(q)$ HS		SSTL		Doyama and Cotterill
60° (I) (eV)	0.207		0.084		• • •
	1.00	(3.00)	1.00	(3.00)	• • •
90° (I)	0.83	(2.49)	0.82	(2.46)	(2.79)
120° (I)	0.64	(1.91)	0.62	(1.85)	(1.94)
180° (I)	0.67	(2.01)	0.67	(2.01)	(2.08)

IV. BINDING ENERGIES OF SMALL POINT-DEFECT CLUSTERS

We will apply the effective interaction potentials between vacancies and impurity atoms to the study of small clusters which play an important role in experiments, such as quenching, annealing, aging, diffusion, irradiation damage, and mechanical deformation.[45] The clustering of point defects, however, has not yet been perfectly understood. For instance, the nature of large aggregates of vacancies and the simplest forms, namely the single vacancy and the divacancy, is known to a certain degree by means of experimental techniques; on the other hand, the shape of the intermediate-size clusters and the formation mechanisms are not very well understood. Moreover, the nature of complicated clusters containing both vacancies and impurity atoms has been difficult to investigate directly by experiments.

The general interaction between vacancies and impurity atoms can be expressed as a sum of their effective interaction potentials.[21] We calculate the electronic binding energies of small clusters containing three point defects, which have considerable interest as the initial stage of larger cluster formation, using the HS and SSTL correction factors in the dielectric function. The only configurations considered here are those for which every point defect is the nearest neighbor of at least one other defect. The most general configurations containing three kinds of point defects, *a*, *b*, and *c*, are shown in Fig. 13, where the angles refer to the angles which the two outer point defects subtend at the middle defect. The impurity atoms and different impurity pairs considered here are Zn, Mg, Cu, and Sn and Zn-Mg, Cu-Sn, and Cu-Mg, respectively. The influence of lattice distortions is regarded to be small in Al-Zn alloys where the difference in atomic radii is small (about 3%), while that is supposed to be large in Al alloys with Mg, Cu, or Sn where the atomic difference is large (about 12%, 11%, 18%, respectively). Hence the present calculations are expected to be good for a Zn impurity atom but poor for Mg, Cu, and Sn impurity atoms. The absolute values of the binding energies given here should not be taken too seriously because the effect of lattice distortions has been ignored. However, the relative values due to configurations are considered to be fairly meaningful. Therefore the values of binding energies are given with respect to three isolated point defects and expressed as the ratios to the binding energy of the 60° (I) type hereafter. The negative values also mean the repulsive interaction. We consider the six cases of small point-defect clusters.

The first case is for trivacancies: *a*, *b*, and *c* all denote the vacancies in Fig. 13. There are four possible types of trivacancies, which are the 60° (I), 90° (I), 120° (I), and 180° (I) types. The binding energies of various trivacancies are given in Table VI. We also show the ratios to the divacancy binding energy. The HS and SSTL corrections give different binding energies but similar relative ratios due to configurations. It is noted that the 60° (I) type is much more tightly bound than the other types. The binding energy of the 90° (I) type is approximately smaller than that of the 60° (I) type by only 17%. The binding energies of a 120° (I) and a 180° (I) trivacancy are very close. The 120° (I) type has the smallest binding energy. In addition, the binding energies of 60° (I), 90° (I), and 180° (I) trivacancies are larger but the binding energy of a 120° (I) trivacancy is smaller than double the divacancy binding energy. It is remarkable that these results are well consistent with the theoretical results obtained by Doyama and Cotterill[46] in copper using a Morse potential function and including the effect of lattice relaxation. The present calculations do not, of course, give the activation energy for the conversion between those configurations. However, the results obtained here do also raise the interesting questions: (i) Can the 60° (I) type be easily transformed into the 90° (I) type? (ii) Can the 120° (I) and 180°

(I) types interchange fairly easily? These two questions are of considerable significance to consider the migration mechanism of the trivacancy. Doyama and Cotterill[46] suggested that case (ii) could have a conversion energy as low as the activation energy for the motion of a divacancy.

The second is for the two vacancies-impurity complexes: *a* and *b* denote the vacancies and *c* denotes the impurity atom in Fig. 13. There are seven possible types of two vacancies-impurity complexes which have been discussed by Doyama.[47] Binding energies of these complexes are given in Table VII. The binding energies are also given with respect to two neighboring vacancies and an isolated impurity atom. The 60° (I) type is much more tightly bound and the 120° (II) type is less tightly bound than the other types except a Sn impurity atom, for which the 120° (I) or 180° (I) type is more tightly bound and the configurations of type II may be generally difficult to form because of the negative binding energies. Third, we consider the complexes containing a vacancy denoted by *a* and two impurity atoms of the same kind denoted by *b* and *c* in Fig. 13. Binding energies of these complexes which have seven possible types are shown in Table VIII. We also give the binding energies with respect to an isolated vacancy and two neighboring impurity atoms of the same kind. The 60° (I) type is generally more tightly bound and the 120° (II) type is also much less tightly bound. It may be noted that the complexes containing Sn impurity atoms have shown the negative binding energies. As seen from Tables VII and VIII, the binding energies of two vacancies-impurity complexes are generally larger than those of complexes containing a vacancy and two same impurity atoms. We consider the complexes containing a vacancy and two impurity atoms of different kinds as the fourth case: *a* denotes the vacancy, and *b* and *c* denote the different impurity atoms in Fig. 13. There are ten possible types in this case. Table IX shows the binding energies of these complexes for three kinds of different impurity pairs and the binding energies with respect to an isolated vacancy and two different neighboring impurity atoms. The configurations of type I give larger binding energies than those of types II and III. The 60° (I) and 90° (I) types for Zn-Mg and Cu-Mg and the 180° (I) type for Cu-Sn are much more tightly bound. The complexes containing Cu-Mg impurity atoms show larger binding energies than the other complexes. It is very interesting to note that the complexes containing a vacancy and Cu-Sn impurity atoms give the binding energies though the complexes containing a vacancy and two Sn impurity atoms all have shown the negative binding energies. This is resulted from the fact that the vacancy-Cu impurity binding energy is comparatively large in

TABLE VII. Binding energies of various two vacancies-impurity complexes in aluminum (eV). Also given are the binding energies with respect to two neighboring vacancies and an isolated impurity atom in parentheses. HS and SSTL denote the correction factors $f(q)$ used.

	Impurity atom											
	Zn			Mg			Cu			Sn		
Type	HS		SSTL	HS		SSTL	HS		SSTL	HS		SSTL
60° (I)	(eV) 0.131	(0.062)	0.041	(0.013)	0.154	(0.085)	0.046	(0.018)	0.159	(0.090)	0.081	(0.053)	0.064	(−0.005)	−0.002	(−0.029)
	1.00	(1.00)	1.00	(1.00)	1.00	(1.00)	1.00	(1.00)	1.00	(1.00)	1.00	(1.00)	1.00	(−1.00)	−1.00	(−1.00)
90° (I)	0.84	(0.66)	0.94	(0.82)	0.78	(0.61)	0.91	(0.76)	0.87	(0.77)	0.79	(0.68)	0.81	(−3.20)	5.87	(−0.65)
120° (I)	0.76	(0.49)	0.81	(0.39)	0.72	(0.49)	0.77	(0.40)	0.71	(0.49)	0.63	(0.44)	1.03	(−0.61)	9.67	(−0.46)
180° (I)	0.77	(0.51)	0.81	(0.55)	0.73	(0.51)	0.83	(0.57)	0.72	(0.50)	0.67	(0.49)	1.06	(−0.28)	9.73	(−0.45)
90° (II)	0.73	(1.00)	0.63	(1.00)	0.77	(1.00)	0.67	(1.00)	0.78	(1.00)	0.81	(1.00)	0.45	(−1.00)	−11.1	(−1.00)
120° (II)	0.47	(1.00)	0.22	(1.00)	0.55	(1.00)	0.30	(1.00)	0.56	(1.00)	0.61	(1.00)	−0.09	(−1.00)	−22.3	(−1.00)
180° (II)	0.48	(1.00)	0.32	(1.00)	0.56	(1.00)	0.39	(1.00)	0.57	(1.00)	0.66	(1.00)	−0.07	(−1.00)	−19.5	(−1.00)

spite of the negative binding energies both between a vacancy and a Sn impurity atom and between Cu-Sn impurity atoms.

Next we consider the small impurity clusters, which is important to understand the early formation of GP zones. In Fig. 13, *a*, *b*, and *c* all denote the same impurity atoms. The binding energies of various small impurity clusters containing three impurity atoms of the same kind are given in Table X. The 60° (I) type is much more tightly bound than the other types, which give almost the same energies, except a Mg impurity atom (SSTL) and a Sn impurity atom (HS). All negative binding energies are found for these two cases. We lastly consider the *A-A-B* impurity clusters containing two impurity atoms of the same kind *A* denoted by *a* and *b*, and another impurity atom *B* denoted by *c* in Fig. 13. Binding energies of various *A-A-B* impurity clusters are presented in Table XI. The difference of the binding energies due to configurations is small for Zn-Zn-Mg clusters. The 60° (I) type is more tightly bound according to the HS correction factor, but all binding energies are nearly zero according to the SSTL one. The HS and SSTL corrections give quite different results for Zn-Mg-Mg clusters: the HS correction gives the binding energies but the SSTL one gives the negative binding energies similar to the Mg impurity clusters. For Cu-Cu-Sn clusters the 180° (I) type is more tightly bound than the other types. All types, however, give the negative binding energies for Cu-Sn-Sn clusters. Therefore the Cu-Sn-Sn impurity cluster may be difficult to form. The 60° (I) type is more tightly bound and the 120° (II) and 180° (II) types are less tightly bound than the other types for Cu-Cu-Mg clusters. On the other hand, the configurations of type II are tightly bound except the 60° (I) type (HS) for Cu-Mg-Mg clusters. The binding energies of Cu-Mg-Mg clusters are larger than those of the Mg impurity clusters.

The HS and SSTL correction factors generally gave different absolute binding energies but almost the same relative order of the binding energies due to configurations. This discrepancy can be somewhat improved if the core radii used are optimized in each case. The 60° (I) type was found to be comparatively tightly bound except a few cases. We consider the effect of a Sn impurity atom on Al-Cu alloys from the present calculations as follows: a Sn impurity atom may form the complexes with two vacancies or both a vacancy and a Cu impurity atom and the vacancy is probably trapped by these complexes. As for the effect of a Mg impurity atom on Al-Zn and Al-Cu alloys, we consider as follows: a Mg impurity atom may form the complexes containing one or two vacancies rather than the clusters containing impurity atoms only. The

TABLE VIII. Binding energies of various complexes containing a vacancy and two impurity atoms of the same kind in aluminum (eV). Also given are the binding energies with respect to an isolated vacancy and two same neighboring impurity atoms in parentheses.

	Impurity atom											
	Zn		Mg		Cu		Sn					
Type	HS	SSTL	HS	SSTL	HS	SSTL	HS	SSTL	HS	SSTL	HS	SSTL
60° (I)	(eV) 0.073	(0.062)	0.014	(0.013)	0.095	(0.085)	0.048	(0.018)	0.122	(0.090)	0.080	(0.053)	−0.022	(−0.005)	−0.027	(−0.029)
	1.00	(1.00)	1.00	(1.00)	1.00	(1.00)	1.00	(1.00)	1.00	(1.00)	1.00	(1.00)	−1.00	(−1.00)	−1.00	(−1.00)
90° (I)	0.87	(1.00)	0.98	(1.00)	0.89	(1.00)	1.08	(1.00)	0.88	(1.00)	0.75	(1.00)	−0.15	(−1.00)	−1.19	(−1.00)
120° (I)	0.84	(1.00)	0.92	(1.00)	0.90	(1.00)	1.10	(1.00)	0.74	(1.00)	0.64	(1.00)	−0.15	(−1.00)	−1.04	(−1.00)
180° (I)	0.85	(1.00)	0.94	(1.00)	0.89	(1.00)	1.09	(1.00)	0.74	(1.00)	0.65	(1.00)	−0.34	(−1.00)	−1.19	(−1.00)
90° (II)	0.71	(0.66)	0.83	(0.82)	0.65	(0.61)	0.19	(0.76)	0.83	(0.77)	0.79	(0.68)	−1.54	(−3.20)	−0.62	(−0.65)
120° (II)	0.57	(0.49)	0.43	(0.39)	0.54	(0.49)	0.06	(0.40)	0.63	(0.49)	0.63	(0.44)	−0.91	(−0.61)	−0.41	(−0.46)
180° (II)	0.59	(0.51)	0.58	(0.55)	0.56	(0.51)	0.12	(0.57)	0.63	(0.50)	0.66	(0.49)	−0.84	(−0.28)	−0.40	(−0.45)

TABLE IX. Binding energies of various complexes containing a vacancy and two impurity atoms of different kinds in aluminum (eV). Also given are the binding energies with respect to an isolated vacancy and two different neighboring impurity atoms, in parentheses.

	Impurity atoms											
	Zn-Mg				Cu-Sn				Cu-Mg			
Type	HS		SSTL		HS		SSTL		HS		SSTL	
60°(I)(eV)	0.086	(0.073)	0.015	(0.015)	0.040	(0.042)	−0.005	(0.012)	0.115	(0.087)	0.042	(0.036)
	1.00	(1.00)	1.00	(1.00)	1.00	(1.00)	−1.00	(1.00)	1.00	(1.00)	1.00	(1.00)
90° (I)	0.87	(1.00)	1.03	(1.00)	0.84	(1.00)	2.04	(1.00)	0.83	(1.00)	0.96	(1.00)
120° (I)	0.86	(1.00)	1.01	(1.00)	1.05	(1.00)	2.48	(1.00)	0.75	(1.00)	0.81	(1.00)
180° (I)	0.86	(1.00)	1.02	(1.00)	1.11	(1.00)	2.78	(1.00)	0.77	(1.00)	0.88	(1.00)
90° (II)	0.76	(0.71)	0.84	(0.84)	0.48	(0.52)	−4.42	(−0.43)	0.82	(0.77)	0.59	(0.52)
120° (II)	0.64	(0.57)	0.48	(0.48)	−0.16	(−0.08)	−6.98	(−1.49)	0.60	(0.48)	0.28	(0.16)
180° (II)	0.65	(0.59)	0.62	(0.62)	−0.14	(−0.06)	−6.42	(−1.26)	0.61	(0.49)	0.35	(0.24)
90° (III)	0.61	(0.55)	0.72	(0.73)	0.70	(0.72)	1.06	(1.86)	0.71	(0.62)	0.90	(0.88)
120° (III)	0.49	(0.41)	0.31	(0.31)	1.05	(1.05)	2.20	(2.33)	0.62	(0.50)	0.75	(0.70)
180° (III)	0.52	(0.44)	0.50	(0.50)	1.09	(1.08)	2.22	(2.34)	0.64	(0.53)	0.82	(0.79)

vacancy will be trapped by such complexes. The present investigation has, of course, given only the electronic binding energies of small clusters. It is necessary for the precise discussion to include the influence of lattice distortions, since the atoms in and around the cluster will be displaced from their regular lattice positions. GP zone formation, spinodal decomposition, and martensitic transformation are very interesting problems for the further study by the electron theory with the lattice relaxation appropriately taken account.

V. CONCLUSIONS

The electronic interactions between vacancies and impurity atoms have been studied using the pseudopotential formulation based on the second-order perturbation theory. The distortions of the lattice around vacancies and impurity atoms are very difficult problems to treat in a complete form at present; these are conventionally neglected in the present calculations. The treatment used here has improved the electrostatic model based on a self-consistent screening potential. The vacancy-vacancy, vacancy-impurity, and impurity-impurity interaction potentials have been calculated for selected four kinds of impurity atoms using three kinds of correction factors for exchange and correlation effects of the conduction electrons in the dielectric function. They are all long range and show Friedel oscillations. The results obtained from the RPA were found to be less reliable. The appropriate including of many-electron effects is quite essential in obtaining realistic results, which has been also demonstrated in the calculations of binding energies between point defects. The discrepancies between the results based on the HS approximation and those obtained from the SSTL approximation would be somewhat less serious if the core radius were optimized in each case. These effective interaction potentials can be applied to the study of many properties of point defects.

We have also calculated the binding energies of a divacancy, 15 kinds of vacancy-impurity pairs, and 18 kinds of impurity-impurity pairs. The results showed the small binding energies, which were well consistent with recent experiments and theoretical calculations previously obtained from the electrostatic model using the screening potentials. The interaction potentials obtained have been applied to the study of small clusters which

TABLE X. Binding energies of various clusters containing three impurity atoms of the same kind in aluminum (eV).

	Impurity atom							
	Zn		Mg		Cu		Sn	
Type	HS	SSTL	HS	SSTL	HS	SSTL	HS	SSTL
60° (I) (eV)	0.034	0.003	0.030	−0.013	0.095	0.081	−0.050	0.007
	1.00	1.00	1.00	−1.00	1.00	1.00	−1.00	1.00
90° (I)	0.73	0.89	0.67	−0.72	0.85	0.75	−0.63	0.31
120° (I)	0.67	0.59	0.68	−0.64	0.66	0.64	−0.63	0.85
180° (I)	0.67	0.70	0.66	−0.67	0.66	0.66	−0.71	0.29

TABLE XI. Binding energies of various clusters containing two impurity atoms of the same kind and an impurity atom of another kind in aluminum (eV).

	Impurity atoms											
	Zn-Zn-Mg		Zn-Mg-Mg		Cu-Cu-Sn		Cu-Sn-Sn		Cu-Cu-Mg		Cu-Mg-Mg	
Type	HS	SSTL	HS	SSTL	HS	SSTL	HS	SSTL	HS	SSTL	HS	SSTL
60° (I)(eV)	0.036	0.001	0.035	−0.005	0.026	−0.007	−0.023	−0.032	0.087	0.039	0.065	0.008
	1.00	1.00	1.00	−1.00	1.00	−1.00	−1.00	−1.00	1.00	1.00	1.00	1.00
90° (I)	0.69	1.80	0.68	−0.92	0.76	1.17	−1.28	−0.52	0.77	0.96	0.70	0.80
120° (I)	0.66	1.40	0.65	−0.96	1.08	1.49	−0.91	−0.45	0.67	0.80	0.56	0.01
180° (I)	0.66	1.60	0.65	−0.94	1.16	1.70	−0.81	−0.40	0.69	0.87	0.59	0.38
90° (II)	0.75	0.40	0.71	−0.23	0.46	−3.90	−0.16	−1.16	0.84	0.49	0.85	1.46
120° (II)	0.69	−1.20	0.73	0.00	−0.24	−5.19	−0.17	−1.04	0.63	0.26	0.85	1.60
180° (II)	0.69	−0.60	0.71	−0.10	−0.24	−4.99	−0.35	−1.16	0.63	0.29	0.85	1.54

play an important role in various experiments. The HS and SSTL correction factors generally gave different binding energies but similar order of the binding energies due to configurations. As a rule, the 60° (I) type was found to be relatively tightly bound. According to the electronic binding-energy calculation, it seems that a Mg impurity atom traps the vacancy forming the complex with one or two vacancies in Al-Zn and Al-Cu alloys, but a Sn impurity atom traps the vacancy forming the complex with two vacancies or both a vacancy and a Cu impurity atom in Al-Cu alloys.

The model used here can explain qualitatively and semiquantitatively the interactions between vacancies and impurity atoms. There remains a lot more interesting theoretical work to be done in the next stage of this field—especially in extending the present calculations to include appropriate lattice distortions around vacancies and impurity atoms, which in this paper we have conventionally ignored.

ACKNOWLEDGMENT

The authors are grateful to Professor R. R. Hasiguti for his continuous interest and encouragement.

[1]N. H. March and J. S. Rousseau, Cryst. Lattice. Defects 2, 1 (1971).
[2]N. H. March, J. Phys. F 3, 233 (1973).
[3]A. Seeger, J. Phys. F 3, 248 (1973).
[4]A. J. Perry, Acta Metall. 14, 719 (1966).
[5]J. Takamura, in *Lattice Defects in Quenched Metals*, edited by R. M. J. Cotterill, M. Doyama, J. J. Jackson, and M. Meshii (Academic, New York, 1965), p. 521.
[6]For example, A. W. Overhauser, Phys. Rev. 90, 393 (1953); R. A. Swalin, Acta Metall. 5, 443 (1957).
[7]For example, D. Lazarus, Phys. Rev. 93, 973 (1954).
[8]H. Kanzaki, J. Phys. Chem. Solids 2, 24 (1957).
[9]J. W. Flocken, Phys. Rev. B 1, 425 (1970).
[10]J. W. Flocken and J. R. Hardy, Phys. Rev. B 1, 2447 (1970).
[11]P. S. Ho, Phys. Rev. B 3, 4037 (1971).
[12]N. H. March and J. S. Rousseau, in *Interatomic Potentials and Simulation of Lattice Defects*, edited by P. C. Gehlen, J. R. Beeler, Jr., and R. I. Jaffee (Plenum New York, 1972), p. 111.
[13]Z. Popovic, J. R. Carbotte, and G. R. Piercy, J. Phys. F 3, 1008 (1973).
[14]S. P. Singhal, Phys. Rev. B 8, 3641 (1973).
[15]P. A. Flinn and A. A. Maradudin, Ann. Phys. (N. Y.) 18, 81 (1962).
[16]R. Bullough and V. K. Tewary, in Ref. 12, p. 155.
[17]For example, L. C. R. Alfred and N. H. March, Philos. Mag. 2, 985 (1957); G. K. Corless and N. H. March, *ibid.* 6, 1285 (1961); N. H. March and A. M. Murray, Phys. Rev. 120, 830 (1960); J. Woster and N. H. March, J. Phys. Chem. Solids 24, 1305 (1963); A. Blandin and J. L. Déplanté, in Metallic Solid Solutions, edited by J. Friedel and A. Guinier (Benjamin, New York, 1963), p. IV-1.
[18]See, for example, *Solid State Physics*, edited by H. Ehrenreich, F. Seitz, and D. Turnbull (Academic, New York, 1970), Vol. 24.
[19]See, for example, Interatomic Potentials and Simulation of Lattice Defects, in Ref. 12, Parts 1, 2, and 3.
[20]R. Yamamoto, O. Takai, and M. Doyama, Phys. Lett. A 43, 247 (1973).
[21]R. Yamamoto and M. Doyama, J. Phys. F 3, 1524 (1973).
[22]O. Takai, R. Yamamoto, M. Doyama, and Y. Hisamatsu, Phys. Lett. A 45, 437 (1973).
[23]W. A. Harrison, *Pseudopotentials in the Theory of Metals* (Benjamin, New York, 1966).
[24]N. W. Ashcroft, Phys. Lett. 23, 48 (1966).
[25]N. W. Ashcroft and D. C. Langreth, Phys. Rev. 155, 182 (1967); 159, 500 (1967); N. W. Ashcroft, J. Phys. C 1, 232 (1968).
[26]J. Hubbard, Proc. R. Soc. Lond. A 240, 539 (1957); L. J. Sham, Proc. R. Soc. Lond. A 283, 33 (1965).
[27]V. Heine and I. Abarenkov, Philos. Mag. 9, 451 (1964).
[28]K. S. Singwi, A. Sjölander, M. P. Tosi, and R. H. Land, Phys. Rev. B 1, 1044 (1970).
[29]W. A. Harrison, Phys. Rev. 131, 2433 (1963).

[30]O. P. Gupta, Phys. Rev. 174, 668 (1968).
[31]Y. Fukai, Phys. Rev. 186, 697 (1969).
[32]M. Taut and G. Paash, Phys. Status Solidi B 51, 295 (1972).
[33]For example, W. A. Harrison, Phys. Rev. 136, A 1107 (1964); W. M. Shyu and G. D. Gaspari, *ibid.* 170, 687 (1968); W. M. Shyu, J. H. Wehling, M. R. Cordes, and G. D. Gaspari, Phys. Rev. B 4, 1802 (1971); R. W. Shaw and V. Heine, *ibid.* 5, 1646 (1972).
[34]C. P. Flynn, Phys. Rev. 125, 881 (1962).
[35]M. Doyama and J. S. Koehler, Phys. Rev. 84, A 522 (1964).
[36]A. D. King and J. Burke, Acta Metall. 18, 205 (1970).
[37]D. R. Beaman, R. W. Bulluffi, and R. O. Simmons, Phys. Rev. 134, A 532 (1964).
[38]D. R. Beaman, R. W. Bulluffi, and R. O. Simmons, Phys. Rev. 137, A 917 (1965).
[39]N. L. Peterson and S. J. Rothman, Phys. Rev. B 1, 3264 (1970).
[40]C. L. Snead, Jr., T. M. Hall, and A. N. Goland, Phys. Rev. Lett. 29, 62 (1972).
[41]H. Kimura and R. R. Hasiguti, Acta Metall. 9, 1076 (1961).
[42]H. Suzuki, M. Kanno, and K. Fukunaga, J. Jpn. Inst. Light Met. 22, 576 (1972).
[43]O. Takai, R. Yamamoto, M. Doyama, and T. Fukusako, Phys. Lett. A 44, 269 (1973).
[44]A. Blandin and J. L. Déplantê, in Ref. 17.
[45]See, for example, *Lattice Defects in Quenched Metals*, edited by R. M. J. Cotterill, M. Doyama, J. J. Jackson, and M. Meshii (Academic, New York, 1965); also *Lattice Defects and Their Interactions*, edited by R. R. Hasiguti (Gordon and Breach, New York, 1967); A. J. Perry, in Ref. 4.
[46]M. Doyama and R. M. J. Cotterill, in *Lattice Defects and Their Interactions*, edited by R. R. Hasiguti (Gordon and Breach, New York, 1967), p. 80.
[47]M. Doyama, Phys. Rev. 148, 681 (1966).